POLYCRYSTAL CONSTITUTIVE MODELING OF ECAP: TEXTURE AND MICROSTRUCTURAL EVOLUTION

I.J. Beyerlein, R.A. Lebensohn and C.N. Tomé

Los Alamos National Laboratory - Los Alamos NM 87545 - USA

Abstract

This paper describes preliminary efforts to understand the grain refinement mechanism during ECAP. We develop a modeling framework for predicting microstructural and texture evolution in nanocrystalline materials during the Equal Channel Angular Pressing (ECAP). A 3D polycrystalline visco plastic self consistent scheme is used to predict the constitutive response and texture of the sample when subjected to this discontinuous process of rotations and shear straining. We consider a 90° die angle and simulate ECAP up to four passes for four processing routes. The model material is a rigid plastic FCC single phase polycrystal and the empirical grain size evolution model considers only the effects of grain shape. Under these assumptions, route A was the most effective and route C the least effective for grain size refinement after four passes. Route Ba was more effective than route Bc. For producing refined equiaxed grains, route Bc was more effective than Ba and A. We find that incorporation of both shape effects and accumulative dislocation effects in the grain size evolution model are necessary before informative comparison with experimental data is possible.

Keywords: four processing routes, texture, grain refinement, self consistent schemes

Introduction

Equal Channel Angular Pressing (ECAP), is so far the only technique that can process ultrafine-grained materials large enough for structural components. Grain refinement can refer to two features, either nanosized dimensions or equiaxed grain shapes or both. To date there are many experimental studies that demonstrate that ECAP can potentially do both, refine the grain size of coarse-grained pure metals and alloys to at least a few hundred nanometers, ~ 0.2 to 0.4 μm [1,2] and produce an equiaxed microstructure.

In the ECAP process, an alloy billet is severely deformed in shear by forcing the material through a die and changing its direction by an angle Φ, typically ranging from as low as 90° to as high as 157.5° (See Fig. 1). The sample undergoes no change in shape and develops the desired refined equiaxed grain structure after so many passes and rotations. The ECA processing route can involve any number of passes through the die and further variations in microstructure happen when rotating the billet either counterclockwise or clockwise. Not all ECAP routes successfully produce materials with a fine-grained, equiaxed nano-structure or superior mechanical properties [3]. In addition, the route most effective in grain refinement differs from study to study, and is also likely to vary depending on the material.

Ultrafine Grained Materials II; Edited by Y.T. Zhu, T.G. Langdon, R.S. Mishra, S.L. Semiatin, M.J. Saran, and T.C. Lowe. TMS (The Minerals, Metals & Materials Society), 2002.

Further advancement of this technology requires the capability to predict the nanocrystalline microstructures (i.e. grain size and grain micro-structure generated via ECAP) and resulting mechanical properties. To begin such a modeling challenge, one must know the distribution of grain sizes and crystallograhic orientations, or texture, in the nanocrystalline material during the process, not just at the end.

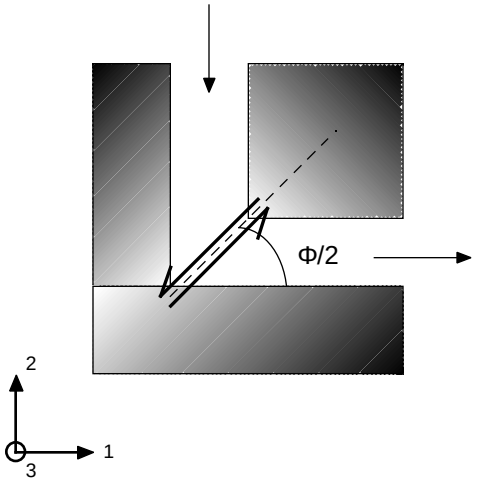

Fig. 1. Schematic of the ECAP process with Φ/2 = 45° die angleand the global coordinate system considered in the model.

ECAP is a discontinuous process, where the orientation of the material texture and the grain morphology change in each pass with respect to the shear plane. Such changes will influence the propensity of aggregate grains to plastically co-deform, subdivide, rotate or slide relative to one another. Knowledge of this texture/shear-plane relationship for every step in the ECAP route will help to explain why some routes are more effective than others in grain refinement. This paper focuses on predicting texture and morphological development associated with the four typical ECAP processing routes.

Modeling texture evolution and grain refinement is accomplished here using the Visco Plastic Self Consistent (VPSC) polycrystal model [4,5], which addresses the problem of large plastic deformation and neglects elastic effects. The VPSC polycrystalline (PX) constitutive model treats each grain as an ellipsoidal visco-plastic inclusion interacting with the effective medium represented by the other grains. This model accounts for plastic anisotropy, and allows the grains to deform differently depending on their relative directional properties with respect to the effective medium. The model predicts overall material response, and texture and grain shape evolution, given the initial grain orientation and shape distribution and constitutive response of the grains.

This work represents a preliminary effort in the development of a model to predict the evolution of microstructural features, such as grain size, hardening and texture, associated with various ECAP processing routes. Here we rely on simple material assumptions to determine the influence of processing route on texture, the geometric hardening associated with texture evolution, and approximate grain refinement information.

Model Description

Our model PX is single phase with an FCC crystal structure. The initial texture of the PX consists of 500 spherical grains with randomly generated discrete orientations, and each with equal volume fraction. Thus the initial texture is uniformly random. We also assume the single crystal follows a rigid plastic constitutive law, without hardening. With this simplistic constitutive relation we can isolate the geometric effects associated with texture evolution from the single crystal hardening associated with dislocation density evolution. Textures resulting from a more realistic single crystal constitutive law, such as one takes into account hardening due to increasing dislocation density or decreasing grain size [6,7], will be generated once the geometric effects are understood.

As suggested previously in [8], we assume simple shear occurs uniformly along the slip plane in each ECAP pass. The magnitude of the shear strain γ along the slip plane $\Phi/2$, has been estimated to be [8]. . . .

$$\gamma = 2\cot(\Phi/2 + \Psi/2) + \Psi \csc(\Phi/2 + \Psi/2) \qquad \text{along } \Phi/2 \qquad (1)$$

For this work, we consider only the case in which the channel die angle Φ is 90° and the angle defined by the outer intersection points, usually denoted Ψ, is 0°. Theoretically this latter situation yields the largest shear strain per pass possible with the ECAP routes, which is

$$\gamma = 2\cot(\Phi/2). \qquad \text{along } \Phi/2 \qquad (2)$$

Since Φ is 90°, (2) results in a shear strain of unity along the 45° slip plane for every pass. We define a global coordinate system (right-handed, orthogonal) which remains fixed during the ECAP process as shown in Fig. 1. Texture and imposed shear are referred to the global system. The rigid body rotations of the sample associated with the different ECAP routes translate into corresponding rigid rotations of the crystallographic texture and the morphology of the grains.

We develop our model framework to simulate the ECAP process for the four common processing routes, routes A, Ba, Bc, and C, as have been designated in the literature. To simulate the rotation schemes applied to the sample for each route, we rotate the sample texture relative to the global coordinate system. Therefore with each ECAP pass, the orientation of the sample texture with the applied slip plane and direction will change. After each pass, the texture is rotated CW $(180 - \Phi) = 90°$ about the 3 axis (from the horizontal to the vertical position) to simulate the re-insertion of the sample into the die entrance. The second rotation depends on the route and pass number. For route A, the texture is not rotated a second time. For route Ba, the texture is rotated about axis-2 CCW 90° after each odd pass and CW 90° after each even pass. For route Bc, the texture is rotated CW 90° about axis-2. For route C, the texture is rotated 180° about axis-2. The first pass is the same for all four routes. The first and second passes are the same for routes Ba and Bc.

We employ an empirical criterion for the grain subdivision process during ECAP. In the model we begin with spherical grains with reference radius one. Under shear deformation, the grain shapes evolve into elongated ellipsoids. We describe each grain by the three ellipsoid axes (given by the eigenvalues of the accumulated distortion tensor): long, medium and short axes with lengths L, M and S, respectively. The grain shape evolution mimics the process that takes place in the real aggregate. However, it is obvious that heavily distorted grains cannot preserve their identity. Rather, through the formation of cell walls and through the local interactions with neighbors, they partition into sub-grains. As a consequence, we implemented in our simulations a simple partitioning criterion based on grain shape. Either or both the

medium and long axes may split. The subdivision criterion is based on two ratios, the ratio of the lengths of the long to short axes, L/S, and the ratio of the medium to short axes, M/S, of the grain. Both the medium and long axes subdivision criteria are satisfied when these ratios achieve a critical value, as follows,

1) $M/S > R/n$ and $L/M < n$ (medium axis split criterion)
2) $L/S > R$ (long axis split criterion) (3)

In the VPSC code, the evolution of the shape of the grains is accounted for in the calculation and is tracked throughout the process. In every deformation step, the criteria (3) are checked for each grain orientation and, when met, the grain shape is split accordingly, while the grain orientation and volume fraction are not modified. The first criterion in (3) is checked first, being independent of the second. If the grain of a given orientation of volume fraction V_f meets the first criterion, the medium axis of the grain is split into n. Then the second criterion is checked. If the second criterion is satisfied, then the long axis of the grain is split into n. Thus if only one of the criteria is satisfied, then the grain is split into n equal size grains, each with the same orientation as the parent grain and with volume fraction V_f/n. If both are satisfied, the grain is split into $2n$ equal size grains each with the same orientation as the parent and each with $V_f/2n$. Essentially, these criteria impose a direct relationship between the shape of the deformed grain (or grain elongation) and grain subdivision. The criteria above are designed such that when the grain becomes say, severally elongated or flat, they are split. In the calculations that follow we assume a fixed critical ratio R of 5 and $n = 2$ for the splitting criteria. Accordingly when the long axis is 5 times the short axis, the long axis is cut in half, and similarly, when the medium axis is 2.5 times the short axis, it is cut in half.

The splitting criteria employed here are empirical and only consider the influence of shape. These criteria are based on previous rolling simulations employing a VPSC scheme that predicts heterogeneous stress states within grains and grain subdivision [9]. In addition, without invoking some sort of splitting scheme, the imposed strains in ECAP are so severe that the aspect ratios of the grains (i.e., long to short axes ratio) become unrealistically large, approximately 30 to 50, and numerical instabilities occur. Certainly other mechanisms are involved in grain subdivision, but it is reasonable to expect that these grains will subdivide or split before they reach such extreme shapes.

Results: Texture and Material Response

This section presents results on the evolution of yield stress, texture and grain refinement using the 3D VPSC code for an FCC single phase polycrystalline aggregate deforming by slip on the (111)[110] systems. The model material was subjected to the four standard ECA processing routes, A, Ba, Bc, and C. By the end of four passes, all four routes complete a cycle and return to the original slip direction and slip plane of the first route. For the purpose of investigating the influence of processing route, applying our model for up to four passes is adequate.

In our model, the ECAP routes are defined by a series of shear passes and rigid sample rotations that result in changes in the relative orientation of the applied shear plane of the current pass with the texture resulting from the previous pass. We record the evolution of the average shear stress, average grain shape and individual grain shape as a function of deformation. We also record the texture after each pass. Figure 2 displays (111) pole figures represented in the 1-2 plane of the absolute coordinate system, after each pass (up to four passes) and before the associated subsequent rotations, for all four routes. The shear plane is 45° from the 1 direction in all these pole figures. Recall that the model material initially had

random texture. By the end of the first pass we predict typical simple shear textures with maximum intensities of about 7 m.r.o.

In subsequent passes, the textures clearly are highly dependent on the processing route and number of passes. In the second to fourth passes, route A induces roughly identical textures after each pass, without a significant change in the intensity. Route C, on the other hand, reverses the shear direction after each pass and, as a consequence, tends to revert the texture to random after the even passes. As a consequence, route C produces the weakest texture. As for routes Ba and Bc, the 90° rotation after each pass introduces shear on different planes each pass. The final result is a rather 'mixed' type of texture with higher intensities than for route A or C. The stronger texture after passes 3 and 4 corresponds to route Ba.

Figure 3 displays the evolution of the shear stress along the slip plane ($\Phi/2$) versus applied shear strain along the slip plane for four passes of each route, A, Ba, Bc, and C, respectively. The first pass is the same for all four routes. The first and second passes are the same for routes Ba and Bc. The shear strain increases by 1 each pass, so $0 < \gamma_{12} \leq 1$ represents the first pass; $1 < \gamma_{12} \leq 2$, the second pass and so on.

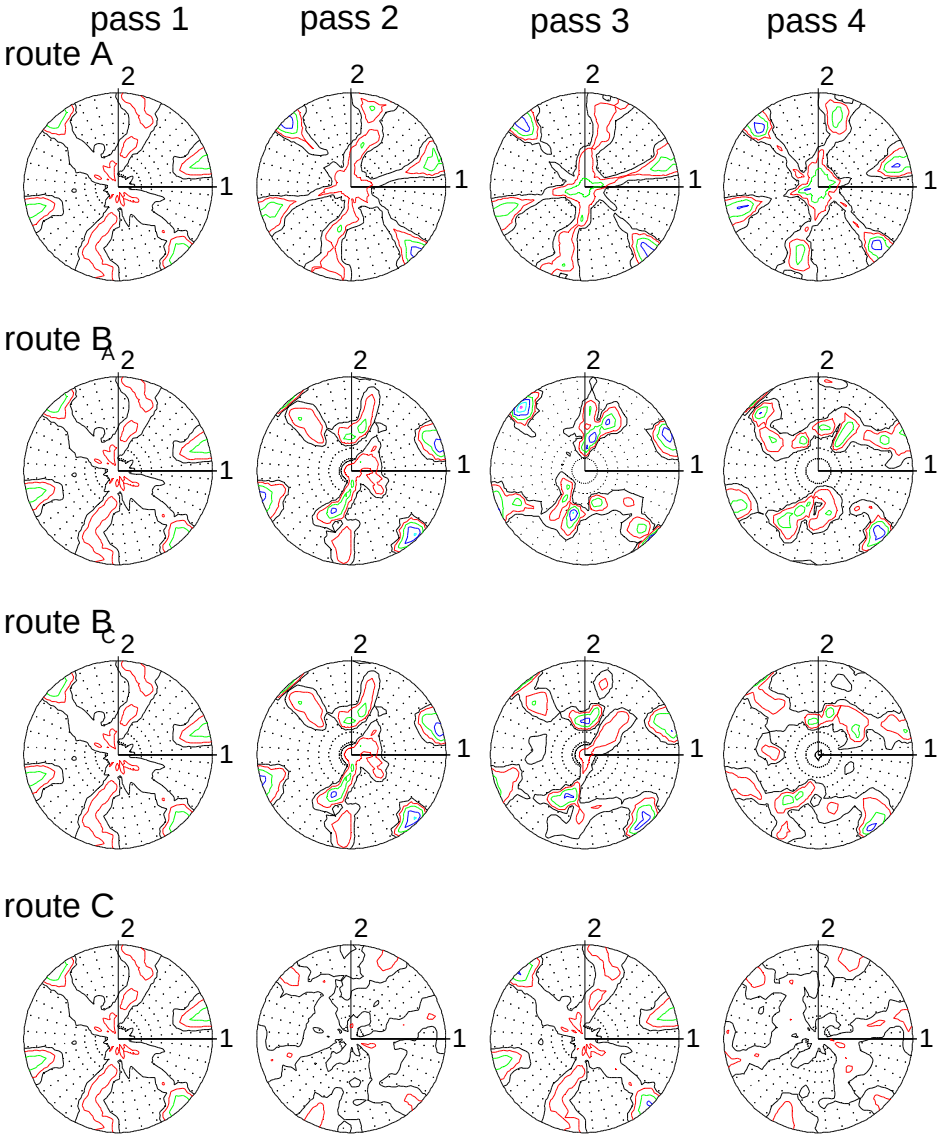

Fig. 2. (111) pole figures after four passes for the four ECAP routes. The intensity levels plotted correspond to 1, 4, 7, 11, 16 multiple of random orientations

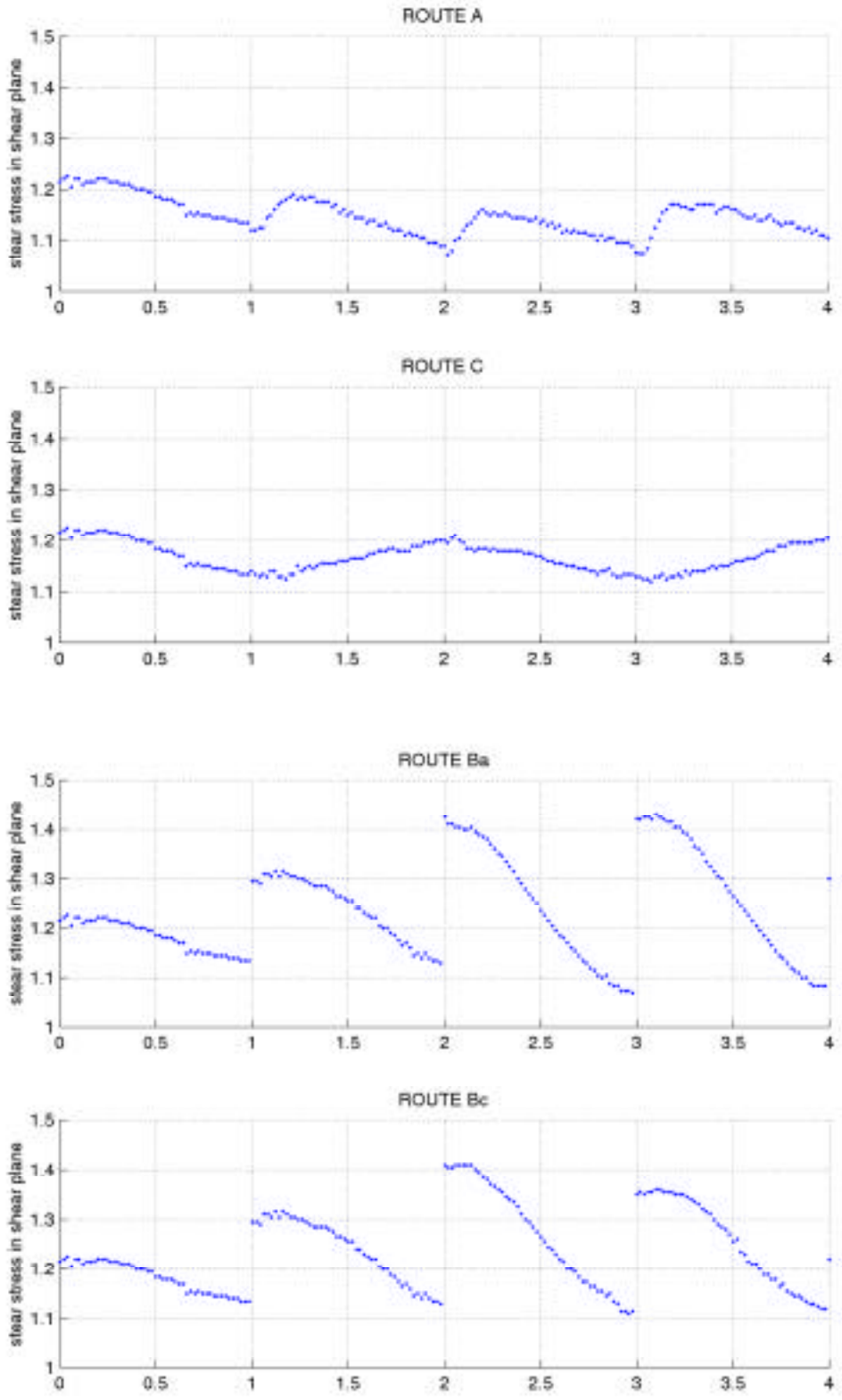

Fig. 3. Shear stress-shear strain response along shear plane of Fig. 1 for the four ECAP routes. A total shear of $\gamma = 1$ is accumulated in each pass.

There are two features of interest: the change in the yield stress from the end of one pass to the beginning of another, and the hardening-softening profile associated with each process. Both features are a geometric consequence of the rigid rotation of the sample (or rather the texture), which changes the grain orientations with respect to the shear plane (remember that the grains are rigid perfectly plastic and do not harden). All ECAP routes lead to changes in this relationship between passes. Hence, discontinuous changes observed in the yield stress between passes will correspond to discontinuous changes in the overall Schmid factor. As shown in Fig. 2, after the first pass the sample develops a strong texture, very different from random. Naturally, in all subsequent passes and under the same applied strain, the sample will tend to develop the same texture as that developed in the first pass and, as a consequence, the sample must make a transition from the rotated texture of the previous pass, which is typically several times random (See Fig. 2). In most cases, this transition to the more favorable orientation forces the grains to reorient along paths which may be geometrically less favorable. This explains the geometric hardening observed at the beginning of several passes in Fig. 3. Apart from a few exceptions, the geometric hardening is eventually followed by a geometric softening once the grains achieve more favorable orientations to accommodate the imposed shear.

Figure 3 shows clearly the effects on material response of rotating the texture with respect to the shear plane between passes. The yield stress discontinuity associated with the discontinuity in the Schmid factor is particularly strong for routes Ba and Bc (see Fig. 3). For route A there is no discontinuity but some hardening takes place in each pass as the texture evolves to the stable one of the first pass. Route C is interesting because the shear, and so the texture, is reversed from pass to pass. As a consequence, the texture tends to go from random to shear, from shear back to random, and from random to shear again, and the yield stress shows softening-hardening-softening accordingly.

Results: Grain Refinement

In all of these ‘four-pass’ routes, the most significant amount of grain elongation occurs before the end of the first pass. Within the first pass, the grain became elongated and the average value of the long grain axis increases until, towards the end of the first pass, the splitting criteria (3) are satisfied and the long axes of the grains subdivide. In subsequent passes, this process of grain elongation and subdivision generally continues and the grains further refine with the exception of route C. In route C, the grain's long axis shorten in the second pass, followed by significant grain elongation by the end of the third pass.

There are two reasons for a decrease in the size of the long and medium- axes: deformation and grain splitting. For instance in route A, grain size reduction clearly occurred by grain splitting. The number of subdivisions in route A was the highest and generally increased with strain within each pass. However for route C, the grain size reduced in the second and fourth passes due to deformation by reverse shear. In the beginning of the third and fourth passes of Bc, the length of the long axes decreased unlike in route Ba. This contraction was due to deformation by redundant strain since there was no associated long axes subdivision.

Our results show that processing route had a significant influence on grain refinement. In Table 1, we report the average grain axes lengths after four passes for each route. Keep in mind that Table 1 reports only the average values. In routes Ba and Bc, we find that the grain sizes (long, medium and short axes) actually follow well a log-normal distribution, after four passes. Microstructures of routes A and C, on the other hand, had a wide dispersion of grain sizes, consisting of many relatively large and small grains. As listed in Table 1, for all routes, the short axes refined the most and the long axes the least. We also estimate the reduction in

grain volume (product of all grain axes) or the ratio of the final-to-initial grain volume V_R , after N passes as

$$V_R(N) = (1/n)^m \text{ where } m = (x_L(N) + x_M(N)) \quad (4)$$

In (4), $x_L(N)$ is the total number of long axis splits and $x_M(N)$ is the total number of medium axis splits per grain after N passes. As shown in Table 1, route A gave the most refinement, followed by routes Ba, then Bc, and finally C with the least amount of grain refinement.

Table 1: Ratios of the final to initial average values of each axis of the grain assuming that when either criteria (3) is satisfied (for $R = 5$), the grain splits in half. Initially all grain axis lengths are unity or all grains are unit spheres.

Route (after four passes)	Long Axis	Medium Axis	Short Axis	Volume	Long/Short
A	0.38	0.16	0.09	5.0×10^{-3}	4.1
Ba	0.49	0.24	0.13	1.3×10^{-2}	3.7
Bc	0.74	0.37	0.23	5.1×10^{-2}	3.2
C	1.04	0.74	0.58	4.0×10^{-1}	1.8

Discussion and Future Work

Our model results agree with the redundant strain theory proposed by Prangnell et al. [10] and trends seen in their FCC Al alloy ECAP studies with $\Phi = 120°$. In route C, the sample texture experiences a severe shear strain that reverses its direction with each pass along the same shear plane. Therefore this route generates redundant strain. Likewise, in route Bc, the sample texture experiences the same reversal after two passes. In our model, this redundant strain essentially hinders grain elongation. When the shear strain experienced by the sample is reversed, most of the grains tend to deform to a lower aspect ratio and therefore they are less likely to meet the split criteria. Since the shear reversal is not sequential in route Bc, this redundancy has less of an effect in route Bc than in route C. In any case there are still many material parameters and deformation phenomena that will need to be implemented into the grain size evolution model before reasonable comparison with experimental data is possible.

The last column of Table 1 reports the long to short axis aspect ratio for the routes as an indication of their effectiveness in producing an equiaxed microstructure. Route A produced mostly elongated grains, even after four passes. Route Bc produced more equiaxed grains than routes Ba or A, which is in agreement with [11]. Route C appears to be the most effective in producing equiaxed grains. However we suspect that results for route C, unlike the other routes, will be more sensitive to our choice of constitutive law (which should account for grain refinement and hardening). This choice allowed the grains to easily lengthen in one pass and shorten in the next in route C, a process that may be impeded by the formation of cells in the grain. Also in route C, the grains did not subdivide significantly after the first pass. Therefore the apparent equiaxed grain structure is a result of the initial spherical grain shape.

Grain refinement occurs by a series of interacting mechanisms, related to shape effects, such as severe deformation, and accumulated dislocation effects, such as subgrain boundary formation, size dependent hardening, and subgrain rotation. The simple criteria employed here superficially accounts for the first effect through the introduction of a fixed critical ratio of $R =$

5 in our splitting criterion. The value selected seemed reasonable based on the results of a more sophisticated VPSC approach (called the N-site model) and its application to rolling simulations [9]. We could have easily altered our empirical splitting critical criteria; however, we propose to direct our future model modifications towards incorporating more microstructure formation and evolution, before informative comparison with experiments can be conducted.

Using our "shape" criteria, route A had the largest number of splits and splits/deformation compared to the other routes. The deformation path or sequences of rotations provided by route A allowed the grains to deform and elongate easily. This route provides more continuity in material mechanical response (i.e. yield stress and equivalent stress) between passes than routes Bc or Ba, yet it is not a continuous deformation process. On the other hand, route C had the least number of splits and splits/deformation. This suggests that significant grain refinement for route C will occur by subgrain, formation, rotation or sliding, rather than by shape effects.

For the purpose of simulation, we use relationship (2) for the shear strain and shear plane direction imposed on the material during the ECAP process, and assume homogeneous deformation throughout the sample. Alternatively, our simulation can be interpreted to apply to a small volume element near the axis of the sample, throughout which deformation can be regarded as homogeneous In reality, the strain distribution is affected by friction between the die and the sample, and varies across the sample as well as along the sample axis. Later we envision transferring this material model into a FE structural analysis that simulates ECAP. Our current constitutive model development efforts begin at the length scale of the polycrystalline aggregate under various loading histories of uniform strain. Further modifications include incorporating sub-cell development governed by a stress/strain-based refinement criteria. Polycrystalline (or rather nanocrystalline) constitutive laws which accurately capture the influence of grain size, texture, and deformation mechanisms will be needed in structural codes which implement structural and boundary conditions existing at a higher length scale.

Acknowledgement

This work was performed under the auspices of the United States Department of Energy (US DOE) and was supported in part by the Division of Materials Science of the Office of Basic Energy Sciences of the US DOE.

Referenece

1. S.X. McFadden, R.S. Mishra, R.Z.Valiev, A.P. Zhilyaev, A.K. Mukherjee, *Nature* **398** (1999) 684-686.
2. R.Z. Valiev et al., "Bulk nanostructured materials from severe plastic deformation", *Prog. Mater. Sci*. **45** (2000) 103-189.
3. Y. T. Zhu and T. C. Lowe, "Observations and issues on mechanisms of grain refinement during the ECAP process.", *Mater. Sci. Engng*. **A291**, 2000, 46-53.
4. U.F. Kocks, C.N. Tomé and H.-R. Wenk, "Texture and Anisotropy", Cambridge Univ. Press, Cambridge (2nd edition, 2000).
5. R.A. Lebensohn and C.N. Tomé, "A Self-Consistent Anisotropic Approach for the Simulation of Plastic Deformation and Texture Development of Polycrystals: Application to Zr Alloys", *Acta metall. Mater*. **41** (1993) 2611-24.
6. P.S. Follansbee and U.F. Kocks, "A Constitutive Description of the Deformation of Copper Based on the Use of the Mechanical Threshold Stress as an Internal State Variable", *Acta metall*. **36** (1988) 81-93.

7. S. Kok, A.J. Beaudoin and D.A. Tortorelli, “A continuum approach to stage IV hardening”, submitted to *Acta Mater*. (2001).
8. Iwahashi et al., "Principle of equal channel angular pressing for the processing of ultra-fine grained materials", *Scripta Mater.* **35** (1996)143-146.
9. R.A. Lebensohn, "N-site Modelling of a 3D Viscoplastic Polycrystal Using Fast Fourier Transform", *Acta mater*. **49** (2001) 2723-37.
10. Prangnell et al., "The effect of strain path on the rate of formation of high angle grain boundaries during ECAE", *Investigations and Applications of Severe Plastic Deformation*. (T. C. Lowe and R. Z. Valiev, eds.) Kluwer Academic Publishers, Netherlands (2000) 65-71.
11. Iwahashi et al., "The process of grain refinement in equal-channel angular pressing", *Acta Mater*. **46** (1998) 3317.